Measuring optical activity with unpolarized light: Ghost polarimetry

Sara Restuccia,[1,*] Graham M. Gibson,[1] Leroy Cronin,[2] and Miles J. Padgett[1]

[1]*School of Physics and Astronomy, University of Glasgow, Glasgow G12 8QQ, United Kingdom*

[2]*WestCHEM, Department of Chemistry, University of Glasgow, Glasgow G12 8QQ, United Kingdom*

(Received 11 August 2022; accepted 9 November 2022; published 1 December 2022)

Quantifying the optical activity of a sample requires the precise measurement of the rotation of the plane of linear polarization of the transmitted light. Central to this notion is that the sample needs to be exposed to light of a defined polarization state. We show that by using a polarization-entangled photon source we can measure optical activity whilst illuminating a sample with unpolarized light. This not only allows for low light measurement of optical activity but also allows for the analysis of samples that would otherwise be perturbed if subjected to polarized light.

DOI: 10.1103/PhysRevA.106.062601

I. INTRODUCTION

The optical activity of a sample, as manifested in the optical rotation of the transmitted light, is quantified by studying its interaction with a linearly polarized beam of light. In particular, when linearly polarized light passes through an optically active sample the plane of polarization is rotated by an amount proportional to the degree of activity and is measured using a polarimeter. The technique is frequently used to measure the concentration or enantiomeric ratio of chiral molecules in solution [1].

In a traditional polarimetry detection scheme, the precision of the measurement increases with the intensity of the light used. This becomes a problem in situations where the intensity of the incident light might cause damage to the sample whose chirality is being probed, or indeed where the light itself may modify the chirality to be measured [2]. A keen interest has therefore been growing in developing low-light quantum detection schemes [3–6]. It is also important to note that traditional polarimetry methods currently in use necessitate the probing light to be linearly polarized as the information on the optical activity is gained by observing the relative change in polarization from before and after it interacts with the sample. Following the growth of nano-optics and photonics, a need has arisen for new methods of studying the optical properties of materials and in particular materials that are affected by polarization, some examples being birefringent and circular dichroic materials [7,8]. In this work we propose an alternative detection scheme with a configuration similar to that which might be used for demonstrating quantum correlations in the form of a Bell inequality [9,10]. In these configurations, polarization-correlated photons produced by parametric down-conversion are employed to probe the chiral solution. We demonstrate that this system can be utilized for measuring the chirality in the low-photon-number regime and show that we are able to measure chirality using unpolarized light.

*sara.restuccia@glasgow.ac.uk

II. EXPERIMENTAL METHOD

The quantum detection scheme proposed in this work uses polarization-entangled photons generated by a spontaneous parametric down-converted (SPDC) source of the type first described by Kwiat *et al.* in their 1999 paper [11]. This is a well-established method where down-converted light is generated using a two-crystal geometry composed of two type-I "sandwiched" 1-mm crystals (with the optic axes perpendicular to one another), pumped by a 190-mW, 355-nm cw laser beam (as shown in Fig. 1). A half-wave plate is employed to orientate the pump beam at 45° with respect to both the optical axes of the sandwiched down-converting crystals, allowing for the SPDC process to be equally likely to occur in either crystal, i.e., generating a coherent superposition of vertically and horizontally polarized photons.

The 710-nm photon pairs generated through the SPDC process are then separated in the far field by a knife-edge prism into two arms of our experimental apparatus (sample arm and reference arm). Each beam then passes through a 1-mm pinhole and interacts with a polarizer before being collected for detection by photomultiplier tube detectors. In particular, we choose detectors with an effective diameter of 5 mm. Although using a detector with a bigger aperture will inevitably lead to the collection of an increased number of background noise events, it allows for the measurement of photons with a wider range of acceptance angles, making the experimental apparatus more resilient to small misalignments that can arise, for example, from swapping the sample cells in and out of the system. In order to minimize the number of detector events that correspond to background light, a 10-nm bandpass filter, centered at 710 nm, is attached to the aperture of each detector and finally the two detectors are connected to a coincidence counter. A coincidence counter is used to record both the single-photon count rates for the pair of detectors and also to measure coincidences as a function of the polarizer angles, thereby enabling, for example, a demonstration of the Bell inequality. In the ghost configuration we typically recorded single-photon count rates of $S \approx 19\,000\ \mathrm{s}^{-1}$ (at the

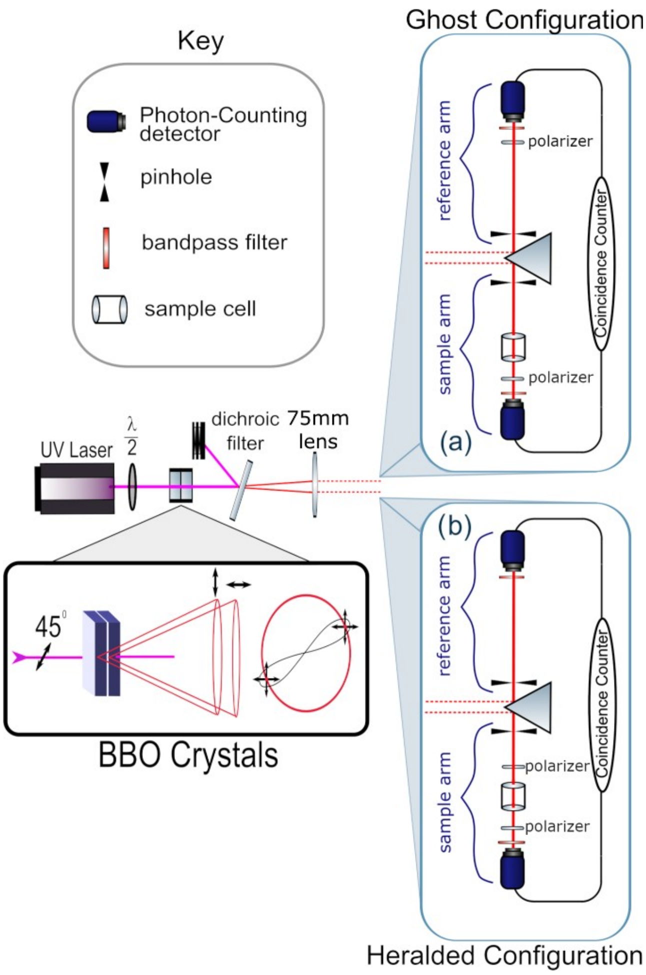

FIG. 1. Experimental setup. A type-I two-crystal geometry SPDC source is employed to generate polarized entangled down-conversion photons. The signal and idler components are then separated in the far field by a knife-edge prism into two arms each containing the following: a 1-mm pinhole, a 10-nm bandpass filter, and a detector. When the system is in the ghost configuration (a), two polarizers are employed, one in each arm of the system. When the system is in the heralded configuration (b), the two polarizers are placed in the same arm (sample arm), one at each side of the sample. For both configurations, coincidences are measured as a function of the relative polarizer angles. When a sample cell containing the chiral solution is placed in the sample arm the optical activity can be measured.

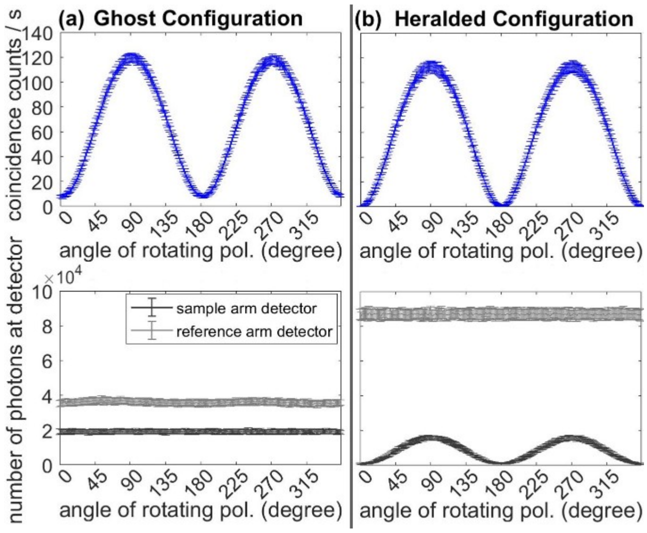

FIG. 2. Experimental results comparing the coincidence and photon counts obtained for both (a) the ghost configuration and (b) the heralded configuration. In the ghost configuration a polarizer is present in both arms and as the light is unpolarized the rotation of the polarizer in the reference arm does not significantly affect the photon count rate; the sinusoidal form is only present in the coincidence counts. In the heralded configuration no polarizer is present in the reference arm (hence the photon count detected is higher) but both polarizers are present in the sample arm on either side of the cell. This will therefore produce a sinusoidal change in both the number of photons detected at the sample detector and the coincidence counts measured.

sample detector) and $R \approx 36\,000\ \mathrm{s}^{-1}$ (at the reference detector) with a corresponding coincidence count rate of $\approx 140\ \mathrm{s}^{-1}$ [Fig. 2(a)]. With a gate time of $\Delta t = 1.523 \times 10^{-9}$ s for the coincidence count rate this gives an accidental background count rate, $acc = S \times R \times \Delta t$, of $\approx 1\ \mathrm{s}^{-1}$.

Drawing inspiration from works of heralded imaging and ghost imaging [12,13], we can now see two ways in which similar optical setups may be used to measure the optical activity of a sample. In a heralded polarimetry configuration we insert both polarizers into the sample arm of the system, on either side of the sample [Fig. 1(b)]. Rotating one polarizer with respect to the other produces a sinusoidal variation in both the photon count rate measured by the detector in the sample arm and in the coincidence count between both detectors [Fig. 2(b)]. In particular, orientation of the transmitted polarization was measured by fitting a sinusoid to 40 runs of the data to calculate both the mean phase (i.e., polarization orientation) and its standard deviation. It is important to note that, compared to the photon count rate at the detector, in the case of the coincidence count the value measured is lower due to the finite heralding efficiency and hence suffers from an increased shot noise, but has the net advantage of being largely background free. In particular, it is well known that in the single mode definition for a coherent state, the shot-noise level is defined by $\langle\sigma\rangle/\sqrt{\langle n\rangle} = 1$, where n is the number of counts and $\langle\sigma\rangle$ is the standard deviation [14,15]. In both the heralded and ghost configurations, the standard deviation increases with the average coincidence counts [Fig. 2]. In the particular case shown in Fig. 2, we chose to measure the coincidence count at each angle of rotation for 12 s.

In the ghost polarimetry configuration [Fig. 1(a)], one polarizer is inserted in each arm (as would be the case for a demonstration of the Bell inequality), but importantly the sample is placed before the polarizer such that it is illuminated by the unpolarized down-converted light. In this case the single photon count rate is independent of the orientation of the polarizer, yet the coincident count rate retains its sinusoidal form [Fig. 2(a)]. In particular, for the ghost configuration we chose to rotate the polarizer located in the reference arm of the setup. As with the case of the heralded configuration,

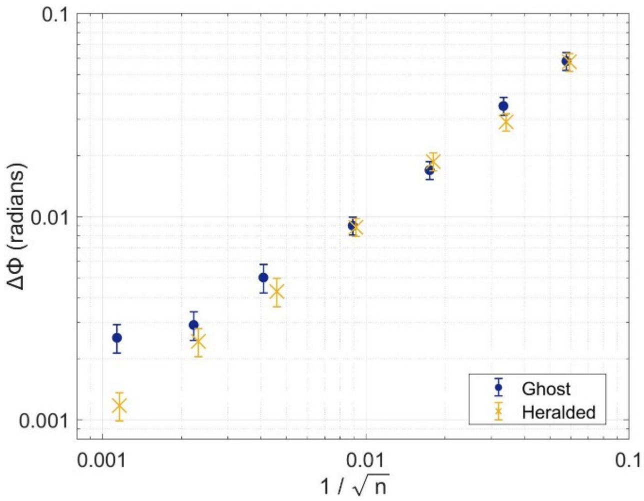

FIG. 3. For both the heralded and ghost configurations we measure the reproducibility of the phase measurement ($\Delta\phi$) as a function of total coincidence counts calculated for a 2π rotation of the polarization. The graph is represented in a log10 scale. As can be seen, the graphs for both the ghost (blue circle) and heralded (yellow "x") configurations have a slope of approximately 1.

the precision of the coincidence measurement in our ghost configuration is also limited by the shot noise on our detected signal.

In both the heralded and ghost configurations, the presence of a chirally active sample in the sample arm will result in a shift of the sinusoidal curves allowing for the direct measurement of the sample optical activity (as can be seen in Sec. IV).

One final question that arises is how we might expect the limiting precision of the measurement to scale with the number of coincidences measured. This particular measurement problem can be considered from various perspectives. For a chiral sample, the incident and transmitted polarization states are nonorthogonal, and nonorthogonal state recognition is an established area [16]. Equivalently, the measurement of the sinusoidal variation in the count rate can be considered as a phase measurement problem. In the latter case the standard quantum limit for the estimation of phase, i.e., using n photons to probe the sample, is given by $\Delta\phi = 1/\sqrt{n}$ [17].

Figure 3 shows the measured reproducibility of the polarization orientation ($\Delta\phi$), as determined by the phase of the sinusoidal count rate as a function of the total number of coincident counts for a full rotation of the sample arm polarizer. The reproducibility of the curve is calculated by measuring the standard deviation of the phase after repeating the full sinusoidal measurement for a given number of times at different values of coincidence counts. The total number of coincidence counts used to measure the sinusoidal curve is regulated by changing the time integration used to calculate each data point in the curve. For the four measurements in graph 3 with the lowest coincidence counts ($1/\sqrt{n} > 0.01$) we repeated the experiment 100 times, while for the remaining data points we repeated the experiment 40 times. It must be noted that, because the polarization vector is bidirectional, a rotation of the polarization state of θ advances the sinusoidal fringes by 2θ so in calculating the phase of the sinusoidal curve we have to correct by a factor of 2. From Fig. 3 we can see that for lower photon numbers the orientation uncertainty closely follows the anticipated relationship with the photon number; i.e., we are shot-noise limited. For very large numbers of photons the uncertainty is higher than expected. We believe this to be due to angular uncertainty introduced by the rotation stages used to rotate the polarizers and for which the uncertainty is ≈1 mrad.

III. EXPERIMENTAL DEMONSTRATION OF THE POLARIZATION CORRELATION

To confirm the entangled nature of our photons and the fidelity of our experimental configuration, we perform a Clauser-Horne-Shimony-Holt (CHSH) Bell inequality test [9,10]. We show that the state generated by our entanglement source violates a Bell inequality of the form

$$|S| \leqslant 2, \tag{1}$$

where

$$S = |E(\theta_S, \theta_R)| + |E(\theta_S, \theta'_R)| + |E(\theta'_S, \theta_R)| + |E(\theta'_S, \theta'_R)| \tag{2}$$

and

$$E(\theta_S, \theta_R) = \frac{C(\theta_S, \theta_R) + C\left(\theta_S + \frac{\pi}{2}, \theta_R + \frac{\pi}{2}\right) - C\left(\theta_S + \frac{\pi}{2}, \theta_R\right) - C\left(\theta_S, \theta_R + \frac{\pi}{2}\right)}{C(\theta_S, \theta_R) + C\left(\theta_S + \frac{\pi}{2}, \theta_R + \frac{\pi}{2}\right) + C\left(\theta_S + \frac{\pi}{2}, \theta_R\right) + C\left(\theta_S, \theta_R + \frac{\pi}{2}\right)}. \tag{3}$$

In Eq. (3), $C(\theta_S, \theta_R)$ is the coincidence count measured when the polarizers in the sample and the reference arm are rotated by θ_S and θ_R, respectively. In particular, a CHSH inequality is maximally violated for the following values: $\theta_S = 22.5^\circ$, $\theta_R = 0^\circ$, $\theta'_S = 67.5^\circ$, and $\theta'_R = 45^\circ$ [18].

As can be deduced from Eqs. (2) and (3), a full measurement of the CHSH test requires 16 measurements corresponding to different orientations of the polarizers. For our S calculation, we therefore choose to calculate each of these measurements for a time integration of ≈3.5 s. Repeating the whole measurement sequence 100 times we obtain a CHSH, S value of 2.39 ± 0.07. It therefore follows that the photons are indeed entangled in polarization, meaning that up to the point of measurement the photon does not have a well-defined polarization. It should be noted that, providing the rotation of the polarization is accounted for, then inserting a chiral sample in our system does not destroy the polarization entanglement of our photons. In particular, with a 1-cm sample present in the system we still obtain a CHSH S value greater than 2; i.e., we measured an S value of 2.46 ± 0.02. The greater precision in the measurement of S stems from two factors: as the presence of a chirally active

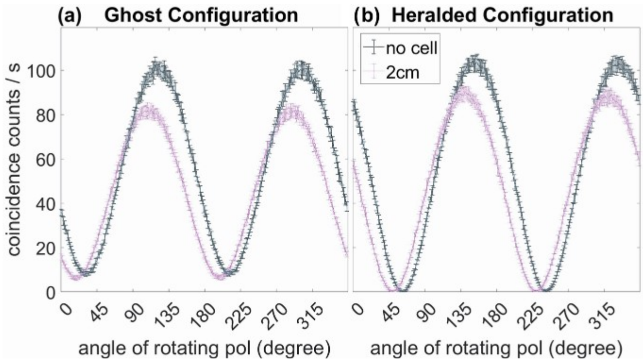

FIG. 4. Comparison between a coincidence measurement taken with no solution in the system and with 2 cm of D-limonene in the system in both the ghost and heralded configurations. The coincidence measurements are shown as a function of polarization angles. In both cases a shift of 25° can be seen due to the chirality of the sample. Note that the coincidence counts with the sample present are lower due to the fact that inserting a glass cell in the system results in a loss of photons. All measurements were obtained with an acquisition time of ≈12.2 s.

sample results in a shift of the sinusoidal curves we choose to measure the full sinusoidal curve instead of only 16 measurements, giving us a more precise measurement of the data point in Eq. (3), and we chose to only take four consecutive measurement sequences but integrate each measurement point for ≈12.2 s. This corresponded to an $n = 203\,000$ coincidence count which corresponded to a phase reproducibility of ≈0.002 rad.

IV. EXPERIMENTAL MEASUREMENTS OF OPTICAL CHIRALITY

Finally, we demonstrate the ability of our heralded and ghost configurations in measuring chirality, in particular, the optical activity of D-limonene. The choice of D-limonene is convenient as it is readily available, highly chiral, and compatible with a comparison to a conventional measurement, i.e., using polarized light. As optical activity scales linearly with sample length, to accurately assess our measurement we repeated the experiment for sample cells of 1, 2, and 5 cm in length. In the case of the ghost configuration, the different cell lengths yielded a shift in the sinusoidal curve of $12.72^\circ \pm 0.62^\circ$, $25.1^\circ \pm 0.77^\circ$, and $69.49^\circ \pm 1.5^\circ$, respectively. In the heralded configuration we measured a shift of $12.14^\circ \pm 0.56^\circ$, $24.54^\circ \pm 0.37^\circ$, and $67.85^\circ \pm 0.41^\circ$ for the 1-, 2-, and 5-cm cells. It must be noted that the known optical rotation for a decimeter tube sample of D-limonene at room temperature is 124° (i.e., 12.4° for a 1-cm cell) [19]. Figure 4 shows the coincidence count rates as a function of the relative orientation of the polarizers in the ghost and heralded configurations with and without the presence of a 2-cm chiral sample in the measurement arm. As expected the measurements of the optical activity of D-limonene for both configurations yield a similar result because the optical activity of D-limonene is independent of the polarization of the light it is probed with; i.e., using nonpolarized light should yield a result similar to that obtained using polarized light and hence we can benchmark the efficiency of our ghost configuration measurement against the heralded configuration. Finally, the error in our measurement is based on repeatability, so it does not take into consideration the precision of the cell length and any error in the path the light takes while going through the cell. This second error is especially important as it is directly related to the length of the cell and how the cell is inserted in the system. Nevertheless, as can be easily seen by our experimental results, not only are our measurements with the ghost and heralded setup consistent with each other and with the known D-limonine optical rotation value but also, as expected, the values increase linearly with cell length.

V. DISCUSSION AND CONCLUSIONS

In this work we propose an alternative detection scheme for measuring the optical rotation of a sample. In particular we propose a quantum configuration known as the Bell inequality and demonstrate that photons in our system are entangled both before and after interacting with a chiral solution (i.e., we can do a CHSH measurement and obtain an S value of $S > 2$). More interestingly we are able to show that we can use the polarized entangled photons to probe a chiral solution with unpolarized light. Even more curiously, we can measure the optical activity of a sample with light that has not interacted with the sample (i.e., ghost polarimetry). We can then benchmark our result against a more conventional measurement of chirality, i.e., using polarized light by converting our system to a heralded setup. As expected the optical activities as measured in the heralded and ghost configurations are statistically consistent with each other as the sample used is not polarization sensitive. We recognize that even at the shot-noise level this approach to measurement is slightly suboptimal since we are using only simple polarizers and only two detectors. This means that we are recording only 25% of the possible coincident counts. If we were instead to use polarizing beam splitters with two detectors in each arm, this would improve the standard deviation of the measurements by a factor of 2 [3]. Nevertheless, beyond our system an interesting manifestation of the implications of quantum entanglement is that our approach allows the measurement of chirality even of samples that would otherwise be perturbed if subjected to polarized light.

All data are available via Ref. [20].

ACKNOWLEDGMENTS

We acknowledge financial support from the EPSRC (U.K. Grant No. EP/S019472/1) and from the Leverhulme Trust (Grant No. RPG-2020-197).

M.J.P. and L.C. conceived the project. The experimental design was by S.R. and M.J.P. with additional input from G.M.G. Results were analyzed by S.R. and M.J.P. S.R. wrote the manuscript with input from all the other authors.

[1] W. J. Lough and I. W. Wainer, *Chirality in Natural and Applied Science* (Blackwell Science, Oxford, 2002).
[2] S.-J. Yoon, J.-S. Lee, C. Rockstuhl, C. Lee, and K.-G. Lee, Experimental quantum polarimetry using heralded single photons, Metrologia **57**, 045008 (2020).
[3] N. Tischler, M. Krenn, R. Fickler, X. Vidal, A. Zeilinger, and G. Molina-Terriza, Quantum optical rotatory dispersion, Sci. Adv. **2**, e1601306 (2016).
[4] V. Cimini, M. Mellini, G. Rampioni, M. Sbroscia, L. Leoni, M. Barbieri, and I. Gianani, Adaptive tracking of enzymatic reactions with quantum light, Opt. Express **27**, 35245 (2019).
[5] J. R. Hance and J. Rarity, Interaction-free polarimetry, arXiv:2207.13539.
[6] S. Magnitskiy, D. Agapov, and A. Chirkin, Ghost polarimetry with unpolarized pseudo-thermal light, Opt. Lett. **45**, 3641 (2020).
[7] S. Magnitskiy, D. Agapov, and A. Chirkin, Quantum ghost polarimetry with entangled photons, Opt. Lett. **47**, 754 (2022).
[8] K. A. Forbes, Optical helicity of unpolarized light, Phys. Rev. A **105**, 023524 (2022).
[9] J. S. Bell, On the Einstein Podolsky Rosen paradox, Phys. Phys. Fiz. **1**, 195 (1964).
[10] J. F. Clauser, M. A. Horne, A. Shimony, and R. A. Holt, Proposed Experiment to Test Local Hidden-Variable Theories, Phys. Rev. Lett. **23**, 880 (1969).
[11] P. G. Kwiat, E. Waks, A. G. White, I. Appelbaum, and P. H. Eberhard, Ultrabright source of polarization-entangled photons, Phys. Rev. A **60**, R773 (1999).
[12] P. A. Morris, R. S. Aspden, J. E. C. Bell, R. W. Boyd, and M. J. Padgett, Imaging with a small number of photons, Nat. Commun. **6**, 5913 (2015).
[13] P.-A. Moreau, E. Toninelli, T. Gregory, and M. J. Padgett, Ghost imaging using optical correlations, Laser Photonics Rev. **12**, 1700143 (2018).
[14] G. Brida, M. Genovese, and I. Ruo Berchera, Experimental realization of sub-shot-noise quantum imaging, Nat. Photonics **4**, 227 (2010).
[15] A. Kuzmich and L. Mandel, Sub-shot-noise interferometric measurements with two-photon states, Quantum Semiclassical Opt.: J. Eur. Opt. Soc., Part B **10**, 493 (1998).
[16] S. Franke-Arnold and J. Jeffers, Unambiguous state discrimination in high dimensions, Eur. Phys. J. D **66**, 196 (2012).
[17] V. Giovannetti, S. Lloyd, and L. Maccone, Quantum-enhanced measurements: Beating the standard quantum limit, Science **306**, 1330 (2004).
[18] P.-A. Moreau, E. Toninelli, T. Gregory, R. S. Aspden, P. A. Morris, and M. J. Padgett, Imaging Bell-type nonlocal behavior, Sci. Adv. **5**, eaaw2563 (2019).
[19] D. R. Lide and G. W. A. Milne, *Handbook of Data on Common Organic Compounds* (CRC, Boca Raton, FL, 1995).
[20] http://dx.doi.org/10.5525/gla.researchdata.1366.